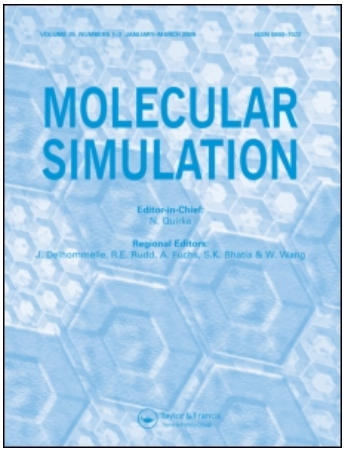

Molecular Simulation
Publication details, including instructions for authors and subscription information:
http://www.informaworld.com/smpp/title~content=t713644482

Methane adsorption in several series of newly synthesised metal-organic frameworks: a molecular simulation study

Qingguo Ye[a]; Shuyun Yan[a]; Dahuan Liu[b]; Qingyuan Yang[b]; Chongli Zhong[b]
[a] Department of Chemical Engineering, Qingdao University of Science and Technology, Qingdao, China [b] Laboratory of Computational Chemistry, Department of Chemical Engineering, Beijing University of Chemical Technology, Beijing, China

Online publication date: 16 August 2010

To cite this Article Ye, Qingguo , Yan, Shuyun , Liu, Dahuan , Yang, Qingyuan and Zhong, Chongli(2010) 'Methane adsorption in several series of newly synthesised metal-organic frameworks: a molecular simulation study', Molecular Simulation, 36: 9, 682 — 692
To link to this Article: DOI: 10.1080/08927021003720538
URL: http://dx.doi.org/10.1080/08927021003720538

Molecular Simulation
Vol. 36, No. 9, August 2010, 682–692

Taylor & Francis
Taylor & Francis Group

Methane adsorption in several series of newly synthesised metal-organic frameworks: a molecular simulation study

Qingguo Ye[a], Shuyun Yan[a], Dahuan Liu[b]*, Qingyuan Yang[b] and Chongli Zhong[b]

[a]*Department of Chemical Engineering, Qingdao University of Science and Technology, Qingdao 266042, China;* [b]*Laboratory of Computational Chemistry, Department of Chemical Engineering, Beijing University of Chemical Technology, Beijing 100029, China*

(*Received 29 October 2009; final version received 22 February 2010*)

In this work, the adsorption of methane in several newly synthesised metal-organic frameworks (MOFs) is studied using grand canonical Monte Carlo simulations. The factors influencing the adsorption behaviour of methane in different series of materials were investigated at low, moderate and high pressures, respectively. The simulation results show that the isosteric heat of adsorption at infinite dilute, the accessible surface area and the free volume of materials play important roles in methane adsorption, while the main factors are different in different ranges of pressure. These are consistent with the rules obtained from well-studied MOFs by the Snurr group and by Wang, proving that they are applicable to the newly synthesised MOFs. Based on these, the influencing factors were further discussed by classifying the MOFs through the pore topology, and it was found that the pore topology should not be ignored when performing efficient modifications of MOFs at moderate and high pressures. This work may provide useful information to design novel MOFs with high methane uptake in the future.

Keywords: newly synthesised metal-organic frameworks; CH_4 adsorption; grand canonical Monte Carlo; pore topology

1. Introduction

With the development of the automobile industry, the interest in natural gas as a kind of vehicular fuel has grown considerably. Natural gas, which primarily consists of methane, is a valuable alternative fuel with advantages in comparison with gasoline, such as low cost and clean-burning characteristics [1,2]. However, its application has been impeded by the absence of safe and economical techniques for storage. Therefore, special attention was paid to develop new storage mediums with high performance.

Recently, a new class of porous materials, metal-organic frameworks (MOFs), has been synthesised and structurally characterised. These materials have shown potential applications in gas storage, separations and catalysis, due to the high porosity, high adsorption capacity and thermal stability [3–6]. Some of the MOFs show high capacity for methane storage, and comparative molecular simulation study has been performed by the Snurr group [7] and by Wang [8] to discuss the main factors in determining methane uptake. Moreover, they both studied the complex interplay of the surface area, free volume, the strength of the energetic interaction and the pore size. More recently, with the development of the synthesis technique, several series of MOFs with different topologies have emerged and shown improved methane uptake capacity [9–15]. However, the adsorption character of methane in these MOFs is not quite clear up to now, and it is valuable to check whether the results obtained from the well-studied MOFs are applicable to these newly synthesised materials.

Therefore, a systematic simulation study was performed in this work on the adsorption of methane in several newly synthesised series of MOFs with different topologies, such as M_2(dhtp) [9,10], UMCMs [13,14], Zn-MOF [15] and ZIFs [16,17]. M_2(dhtp) is also called CPO-27-M (M = Mg, Mn, Co, Ni, Zn) [11,12]. Zn_2(dhtp), known as MOF-74, was first reported, by Yaghi and co-workers [18]. Co_2(dhtp) and Ni_2(dhtp) were prepared by Dietzel et al. [19,20].

The purpose of this paper is to explore the factors that affect the adsorption behaviour of methane at different ranges of pressure, providing more comprehensive understanding of MOFs as the storage medium of methane.

2. Models and simulation methods

2.1 MOF model

In this computational study, the guest-free framework structures of the selected MOFs were constructed from their corresponding experimental single-crystal X-ray diffraction (XRD) data using Materials Studio Visualizer [21] and are shown in Figure 1. M_2(dhtp) (M (metal) = Mg, Mn, Co, Ni, Zn; dhtp = 2,5-dihydroxyterephthalate) has the same topology with M linked by dhtp linkers [9,10]. ZIFs have

*Corresponding author. Email: liudh@mail.buct.edu.cn

ISSN 0892-7022 print/ISSN 1029-0435 online

DOI: 10.1080/08927021003720538
http://www.informaworld.com

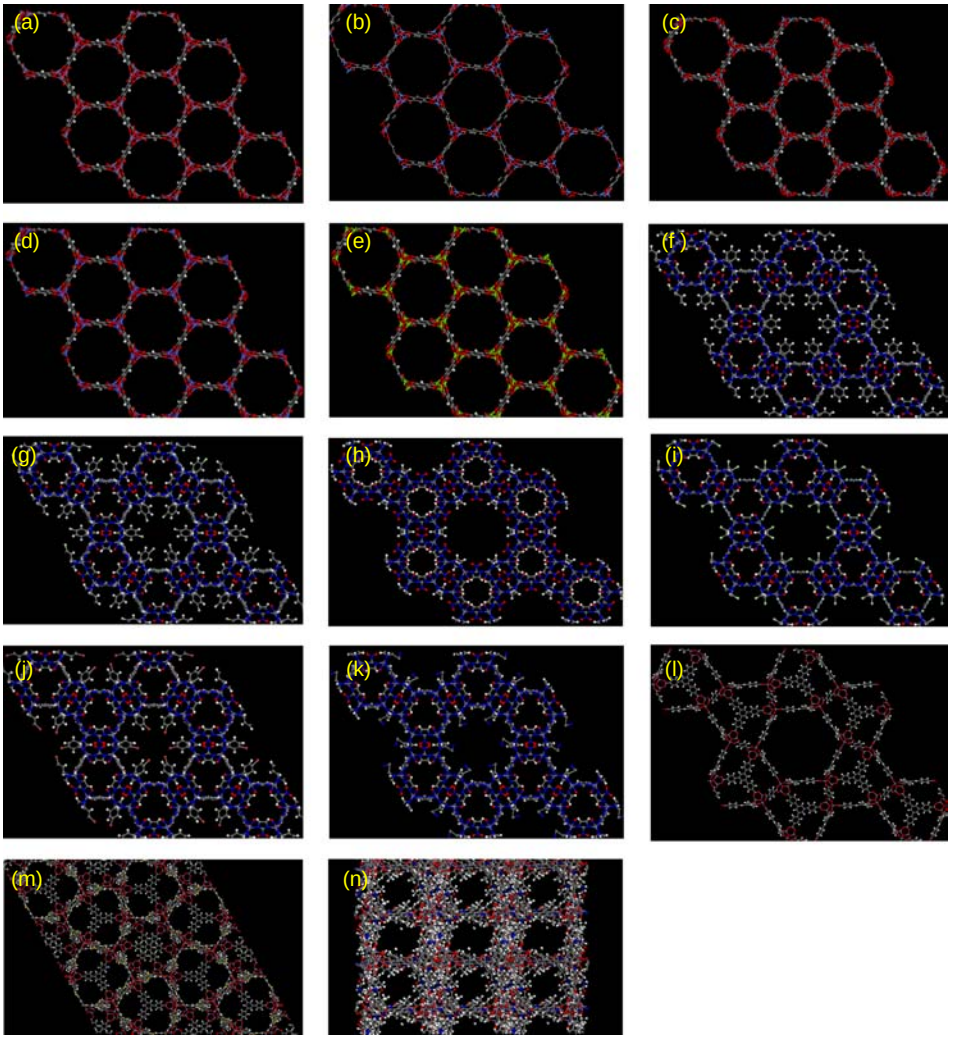

Figure 1. Crystal structures of newly synthesised MOFs used in the simulations: (a) Mn_2(dhtp), (b) Ni_2(dhtp), (c) Zn_2(dhtp), (d) Co_2(dhtp), (e) Mg_2(dhtp), (f) ZIF-68, (g) ZIF-69, (h) ZIF-70, (i) ZIF-80, (j) ZIF-81, (k) ZIF-82, (l) UMCM-1, (m) UMCM-2 and (n) Zn-MOF (Mg, green; Zn, grey-blue; Mn, purple; Ni, light blue; Co, blue; Cl, light green; Br, orange; O, red; C, grey; N, blue; S, yellow; H, white) (colour online).

the same primitive topology with Zn linked by different imidazolate/imidazolate-type linkers [16,17]. UMCMs (UMCM-1 and UMCM-2) [13,14] have cage-like structures with different linkers. Zn-MOF [15] comprises dicarboxylated organic ligands as struts and Zn(II)-containing clusters as nodes. The details of properties for all MOFs are shown in Table 1. The accessible surface area (S_{acc}) and total free volume (V_{free}) of each material were estimated using the atom volumes and surfaces calculations within the Materials Studio package [18]. A probe molecule with the diameter equal to the kinetic diameter of methane (3.8 Å) was used to determine the accessible surface area, whereas the total free volume not occupied by the framework atoms was calculated by a probe size of 0.0 Å.

2.2 *Force field*

In the present work, methane ($\sigma_{CH_4} = 0.373$, $\varepsilon_{CH_4}/k_B = 148.0$ K) is described as a single Lennard-Jones (LJ) interaction site model using the TraPPE force field [22]. The potential parameters for the framework atoms in MOFs were taken from the universal force field of Rappé et al. [23], as shown in Table 2. The sets of force fields have been successfully employed to depict the adsorption [24,25], diffusion [26,27] and separation [28,29] of several light gases and their mixtures in MOFs.

2.3 *Grand canonical Monte Carlo simulation details*

Grand canonical Monte Carlo (GCMC) simulations were employed to calculate the adsorption of methane in all

Table 1. Properties of the MOFs investigated in this work.[a]

Material	Space group	Porous shape	d^{b}_{pore} (Å)	$q^{0\,c}_{st}$ (kJ/mol)	ρ_{crys} (g/cm^3)	S_{acc} (m^2/g)	V_{free} (cm^3/g)
Mg_2(dhtp)	$R\bar{3}$	One-dimensional channel	13.4	14.6	0.91	1534.2	0.71
Mn_2(dhtp)	$R\bar{3}$	One-dimensional channel	13.8	13.4	1.08	1319.8	0.62
Co_2(dhtp)	$R\bar{3}$	One-dimensional channel	13.6	13.8	1.17	1216.4	0.56
Ni_2(dhtp)	$R\bar{3}$	One-dimensional channel	13.5	14.2	1.20	1153.7	0.54
Zn_2(dhtp)	$R\bar{3}$	One-dimensional channel	13.5	14.7	1.23	1146.7	0.53
ZIF-68	$P6_3/mmc$	Cages	10.3	18.7	1.03	1001.5	0.59
ZIF-69	$P6_3/mmc$	Cages	7.8	20.5	1.00	607.2	0.57
ZIF-70	$P6_3/mmc$	Cages	15.9	20.0	0.77	1788.5	0.87
ZIF-80	$P6_3/mmc$	Cages	9.8	16.7	1.07	1061.2	0.60
ZIF-81	$P6_3/mmc$	Cages	7.4	20.2	1.15	491.4	0.49
ZIF-82	$P6_3/mmc$	Cages	12.3	16.6	0.80	1569.5	0.81
UMCM-1	$P6_3/m$	Cages	26.0/31.0	9.8	0.37	4484.8	2.31
UMCM-2	$P6_3/m$	Cages	16.0/18.0/30.0	9.54	0.38	4487.4	2.24
Zn-MOF	$P2(1)/c$	Pore	19.6	13.0	0.50	3403.7	1.58

[a] Obtained from the Materials Studio package [18]. [b] Obtained from the XRD [9–17]. [c] Obtained from the simulations in this work.

MOFs. A cut-off radius of 12.8 Å was applied in the LJ interactions. For each point on the isotherm, 2×10^7 Monte Carlo steps were performed. The 1×10^7 steps were used for the GCMC simulation equilibrium. The isosteric heat of adsorption q_{st} was calculated from:

$$q_{st} = RT - \frac{\langle U_{ff}N\rangle - \langle U_{ff}\rangle\langle N\rangle}{\langle N^2\rangle - \langle N\rangle\langle N\rangle} - \frac{\langle U_{sf}N\rangle - \langle U_{sf}\rangle\langle N\rangle}{\langle N^2\rangle - \langle N\rangle\langle N\rangle}, \quad (1)$$

where R is the gas constant, N is the number of molecules adsorbed and $\langle\,\rangle$ indicates the ensemble average. The first and second terms are the contributions from the molecular thermal energy and adsorbate–adsorbate interaction energy, U_{ff}, respectively. The third term is the contribution from the adsorbent–adsorbate interaction energy, U_{sf}. A detailed description of the simulation methods can be found in [30] and our previous work [31]. The isosteric heat of adsorption at infinite dilute q^0_{st} was extrapolated from a series of GCMC simulations at low-pressure region.

Table 2. LJ potential parameters for CH_4 and the MOFs used in this work.

Atom/molecule	σ (nm)	ε/k_B (K)
CH_4	0.37	148.0
MOF_Mg	0.27	55.8
MOF_Zn	0.25	62.4
MOF_Mn	0.27	6.5
MOF_Co	0.26	7.0
MOF_Ni	0.25	7.5
MOF_C	0.34	52.8
MOF_N	0.33	34.7
MOF_H	0.26	22.1
MOF_O	0.31	30.2
MOF_S	0.36	137.9
MOF_Cl	0.35	114.2
MOF_Br	0.37	126.2

3. Results and discussion

3.1 Validation of the force field

To study the adsorption of methane in the MOF materials, the force field should be reliable. Therefore, GCMC simulations were performed to calculate the adsorption isotherms of CH_4 in M_2(dhtp) and ZIFs, which have experimental data [10,17]. The results in M_2(dhtp) and ZIF-82 are displayed in Figure 2, as examples. Figure 2 shows that the predicted results of ZIF-82 are in better agreement with the experimental data than those in M_2(dhtp), due to the former occuring in lower pressure. However, the simulation results in M_2(dhtp) are in good agreement with the experimental data at low pressure. This may be due to the fact that the degree of simulation fluctuation is stronger at high pressures, as well as the solid may have some defects in experiment. Therefore, the force field adopted in this work is reliable and can be applied to other materials.

3.2 Prediction of CH_4 adsorption isotherms in MOFs up to 10.0 MPa

The excess adsorption isotherms in these MOFs at 298 K are presented in Figure 3 in both gravimetric and volumetric units with pressure up to 10.0 MPa. Generally speaking, M_2(dhtp) displays the largest excess adsorption amount per volume of sorbent, while UMCMs show the highest adsorption amount in terms of gravimetric uptake. The behaviour observed in each series of materials is quite similar. It is worth noticing that the intersection of the adsorption isotherms existed among the different series of materials. It may be attributed to

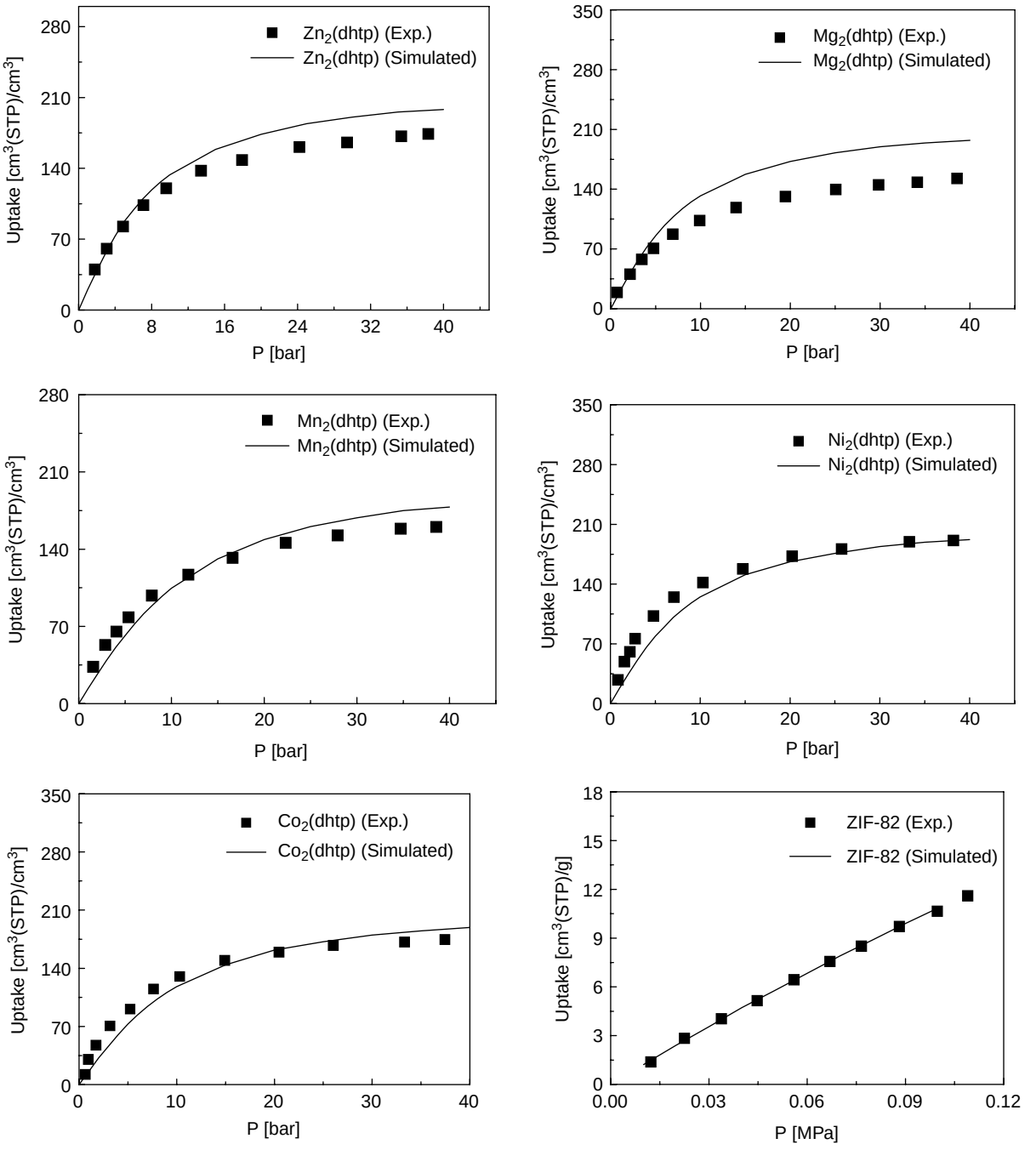

Figure 2. Comparison of simulated and experimental adsorption isotherms of CH_4 in Zn_2(dhtp), Mg_2(dhtp), Mn_2(dhtp), Ni_2(dhtp), Co_2(dhtp) and ZIF-82 at 298 K.

the interplay of various factors at different pressure regions [7,8,31,32], promoting the detailed discussion on these factors in the following sections.

3.3 Various factors at different pressure regions

As shown in Figure 2, the adsorption behaviour of methane in different MOFs is complex at different ranges of pressure. Thus, it is useful to perform a systematic study on the relationships between the methane adsorption capacity and the various influencing factors, which is useful to guide future design of MOFs with high CH_4 uptake.

3.3.1 Moderate pressure

Since, in practical applications, 3.5 MPa is considered as suitable and safe condition for methane storage, some

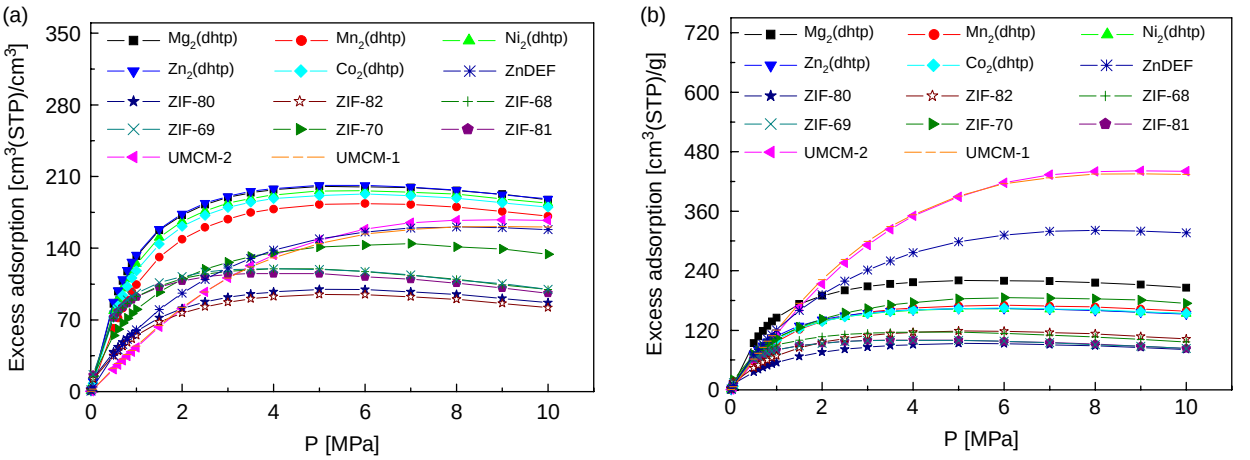

Figure 3. Simulated excess adsorption isotherms of CH_4 in MOFs at 298 K as a function of pressure: (a) volumetric capacity and (b) gravimetric capacity.

main factors influencing the adsorption storage of the materials were examined first at 3.5 MPa and 298 K.

Similar to previous work [7,8,31,32], there is no excellent correlation between the amount adsorbed and the free volume (V_{free}), while the accessible surface area (S_{acc}) shows a nearly linear relation with the adsorption amount, as listed in Figure 4(a), (b). It can be seen from Figure 4(b) that Mg_2(dhtp) has higher adsorption amount than ZIF-82 with similar accessible surface area. This may be due to the different pore topologies and chemical constituents, and, for some ZIFs, the adsorption is near to saturation at that pressure. Therefore, we further discuss the relation between the accessible surface area and the adsorption amount on the basis of classifying materials by the pore topologies (see Table 1 and Figure 1). Figure 4(c) displays the relationship in the materials with channel pore, such as M_2(dhtp) [9,10] and CPLs [8]. To draw a comparison, the results in IRMOFs [8] with cubic or cuboid topology are shown in Figure 4(d). The materials with other structures (ZIFs, UMCMs, Zn-MOF, Cu-BTC, $Cu(SiF_6)(bpy)_2$ and $Cu(GeF_6)(bpy)_2$) are shown in Figure 4(e). Obviously, for the materials with similar pore topology, there is an excellent relation between the accessible surface area and the adsorption amount. By comparing the slopes of correlated line in Figure 4(c)–(e), it can be found that, for the MOFs with channel pore, the increment of adsorption amount is largest with the increase of S_{acc} in all materials studied in this work. That is to say, this kind of MOFs may be more suitable for modification to improve the methane storage capacity through increasing S_{acc}.

3.3.2 *Low pressure*

From the previous works on the gas adsorption in MOFs [7,8,31,32], at low pressure, materials with the strongest enthalpy interactions with molecules adsorbed show the highest level of adsorption capacity. Thus, we also checked the dependency of CH_4 adsorption amount on the isosteric heat of adsorption at infinite dilute (q_{st}^0) for all the series of newly synthesised MOFs at low pressure ($P = 0.05$ MPa), as shown in Figure 5(a). The results indicate that there is obvious linear correlation between them for all the MOFs studied in this work, which has also been found in the well-studied MOFs [8,31,32]. Generally speaking, the higher the isosteric heat of adsorption at infinite dilute, the higher the methane adsorption capacity. However, there is no obvious correlation with the adsorption amount against the other properties of MOFs.

In addition, the relation between q_{st}^0 and pore size of materials was also studied. As can be seen from Figure 5(b), though the value of q_{st}^0 depends on several properties of materials, such as pore size, the framework topology, constituent, atom types and wall chemistry [7,8,31,32], the general trend is that q_{st}^0 decreases with the increasing of pore size.

3.3.3 *High pressure*

Considering that some MOFs are not saturated for methane adsorption at moderate pressure, the factors influencing the amount adsorbed at high pressure ($P = 10.0$ MPa) were further studied for these new materials. By examining the adsorption amount vs. the properties of MOFs, only the free volume and accessible surface area have a nearly linear relation with the capacity of gas storage, as shown in Figure 6(a), (b). It can be seen from Figure 6(a), the methane adsorption capacity of M_2(dhtp) (in red circle) is higher than ZIFs with similar free volume. This is mainly due to the fact that M_2(dhtp) has one-dimensional channel-like pores with less blocking end groups than those in ZIFs, such as nIM and cnIM, as shown in Figure 1(a), (b). Therefore, the relation between the free volume and the

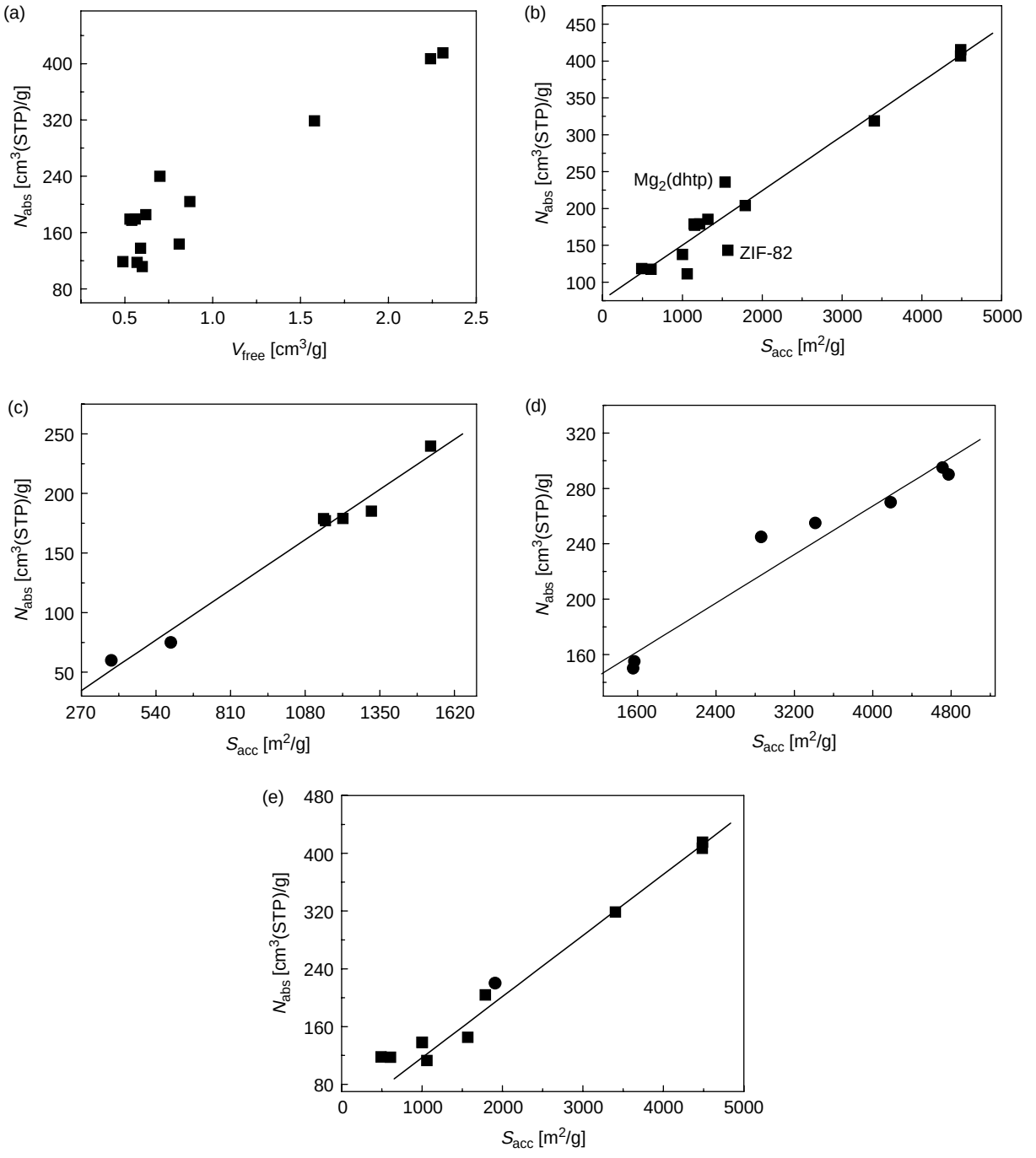

Figure 4. The amount of adsorbed methane at 3.5 MPa vs. (a) the free volume for all the MOFs studied in this work, (b) the accessible surface area for all the MOFs studied in this work, (c) the accessible surface area for the MOFs with channel pore, (d) the accessible surface area for the MOFs with cubic or cuboid pore and (e) the accessible surface area for the MOFs with other pore topology (■, the materials studied in this work; ●, obtained from [8]).

adsorption amount is also investigated based on the pore topology, and the results are listed in Figure 6(c)–(e). It is obvious that there are improved correlations compared to that in Figure 6(a). For the MOFs with channel pore, the increment of adsorption amount is largest with the increase of V_{free} in all the MOFs studied in this work, by comparing the slopes of correlated line in Figure 6(c)–(e). This is similar to that in Figure 4(c)–(e).

The above results indicate that the packing effects are evident at high pressure, and the free volume and the accessible surface area of MOFs become the leading factors for the adsorption capacity, which is consistent

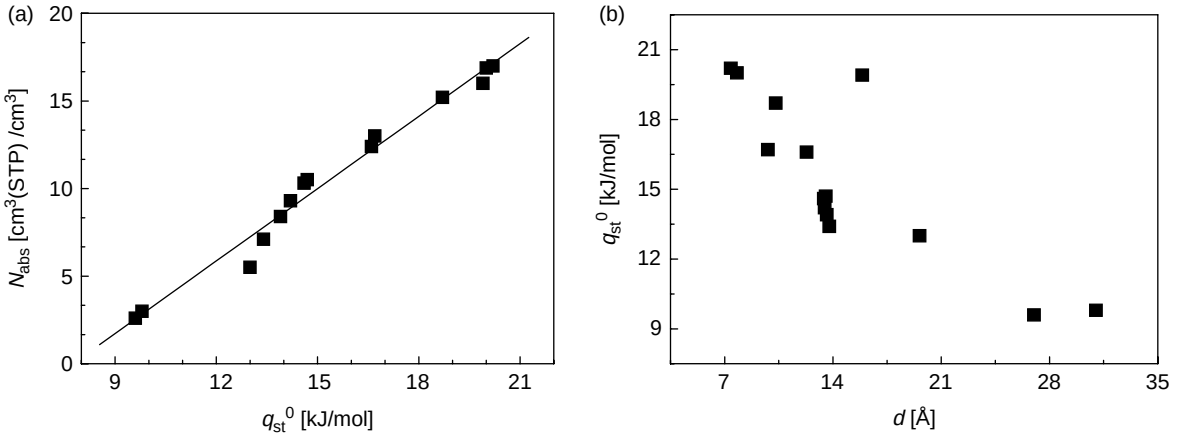

Figure 5. The amount of adsorbed methane at 0.05 MPa vs. (a) the isosteric heat of adsorption at infinite dilute. (b) The isosteric heat of adsorption at infinite dilute vs. the size of pores in MOFs.

with the results obtained by the Snurr group [7] and Wang [8]. In addition, the effect of pore topology should not be ignored at high pressure when designing the MOFs with high performance.

3.4 CH_4 adsorption sites

The knowledge of adsorption sites of gas molecules in MOFs is important in understanding the adsorption mechanism. Therefore, in this work, the centre of mass (COM) probability distributions of adsorbed methane in these newly synthesised MOFs are investigated at different pressures, in order to be helpful for the modification of these materials with improved CH_4 adsorption capacity.

Figure 7 displays the CH_4 adsorption in Mg_2(dhtp) at three different pressure regions, as an example of the series of M_2(dhtp). At low pressure, CH_4 molecules are mainly adsorbed near the Mg clusters (Figure 7(a)), which are the most favourable energetic adsorption regions due to the high concentration of framework atoms and high strength of the interactions. This is similar to the finding of Wu et al. [10]. With the increase in pressure, more and more molecules are adsorbed near the metal clusters and some of them distribute along the organic linkers. Few CH_4 molecules begin to appear in the centres of the channel, as shown in Figure 7(b). With further increasing pressure, the centres of the channel were occupied by more and more CH_4 molecules (Figure 7(c)) until the saturated adsorption amount was reached.

The COM probability distributions of CH_4 adsorbed in ZIF-82 are shown in Figure 8 as an example of ZIFs. Similar to CO_2 [33], at low pressure, CH_4 molecules are mainly adsorbed in the small pores formed by the nIm linkers, with a slight accumulation in other regions of the frameworks (Figure 8(a)). At moderate and high pressures, CH_4 molecules begin to be adsorbed in the large pores as shown in Figure 8(b), (c). This indicates that the small pores formed by nIm linkers are the preferential sites for CH_4 adsorption in ZIFs.

Although the topology is different, at low pressure, CH_4 molecules are mainly adsorbed near the metal clusters in UMCM-2 similar to the situations in Mg_2(dhtp), as shown in Figure 9(a). Increasing pressure induces CH_4 molecules adsorbed near the linker (T^2DC and BTB) and then in the centres of the cavities step by step, as shown in Figure 9(b), (c). It is interesting that CH_4 molecules distribute more uniformly in the cavities of UMCM-2 than in the channel of Mg_2(dhtp).

4. Conclusions

Methane adsorption in several series of newly synthesised MOFs was studied using molecular simulations. Through the comparison of the adsorption behaviour studied in these materials, it is clear that the CH_4 uptake is influenced by the cooperative interplay of the isosteric heat of adsorption, free volume, accessible surface area and the pore topology. Therefore, to synthesise a new desirable material for methane storage, an adsorbent with larger accessible surface area and free volume, low density of framework should be considered. That is to say, the complex interplay of the factors influencing methane adsorption obtained from well-studied MOFs by the Snurr group [7] and by Wang [8] is also applicable to these newly synthesised MOFs, which is likely to be the general rules for design of new MOFs for methane storage. Furthermore, it can be found that, in the MOFs with the same pore topology, there are evident linear relationships between adsorption capacity and the accessible surface area at moderate pressure as well as the free volume at high pressure. Moreover, the MOFs with channel pore may

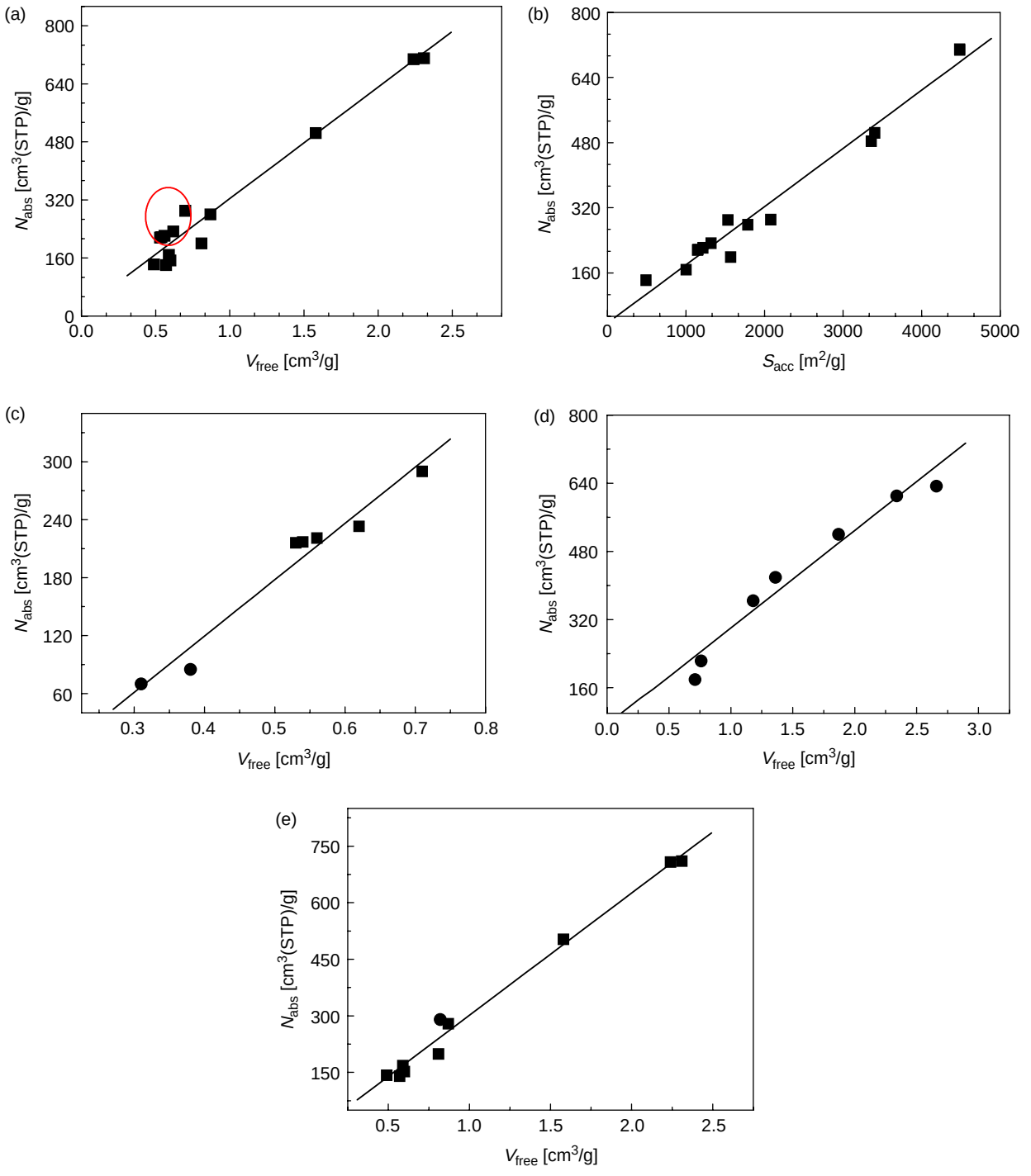

Figure 6. The amount of adsorbed methane at 10.0 MPa vs. (a) the free volume for all the MOFs studied in this work (M_2(dhtp) are in red circles), (b) the accessible surface area for all the MOFs studied in this work, (c) the free volume for the MOFs with channel pore, (d) the free volume for the MOFs with cubic or cuboid pore and (e) the free volume for the MOFs with other pore topology (■, the materials studied in this work; ●, obtained from [8]) (colour online).

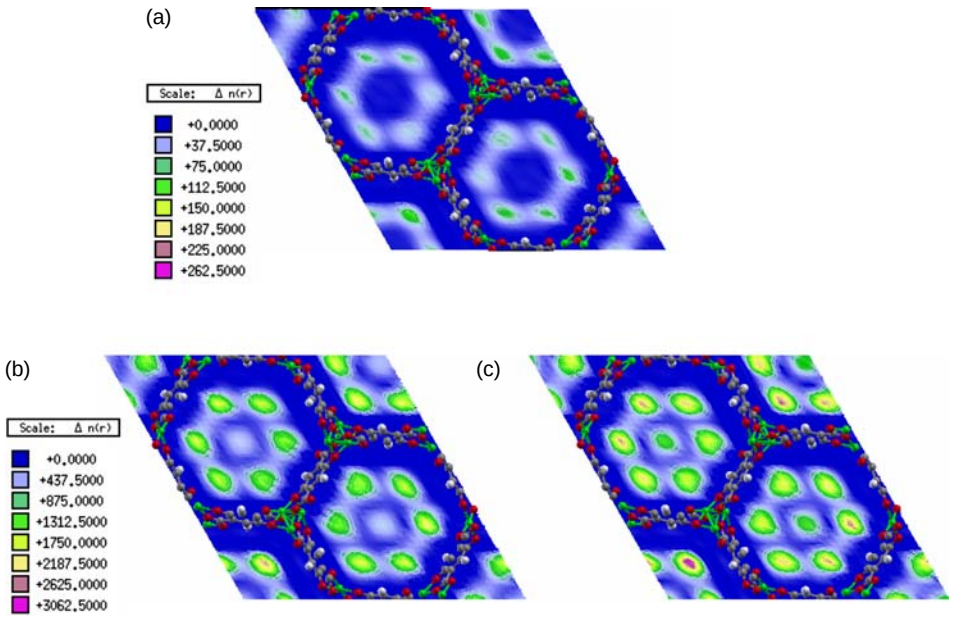

Figure 7. Probability distribution plots of COM of CH_4 in *XY* planes in Mg_2(dhtp) at different pressures: (a) 0.05 MPa, (b) 3.5 MPa and (c) 10.0 MPa (Mg, green; O, red; C, grey; H, white) (colour online).

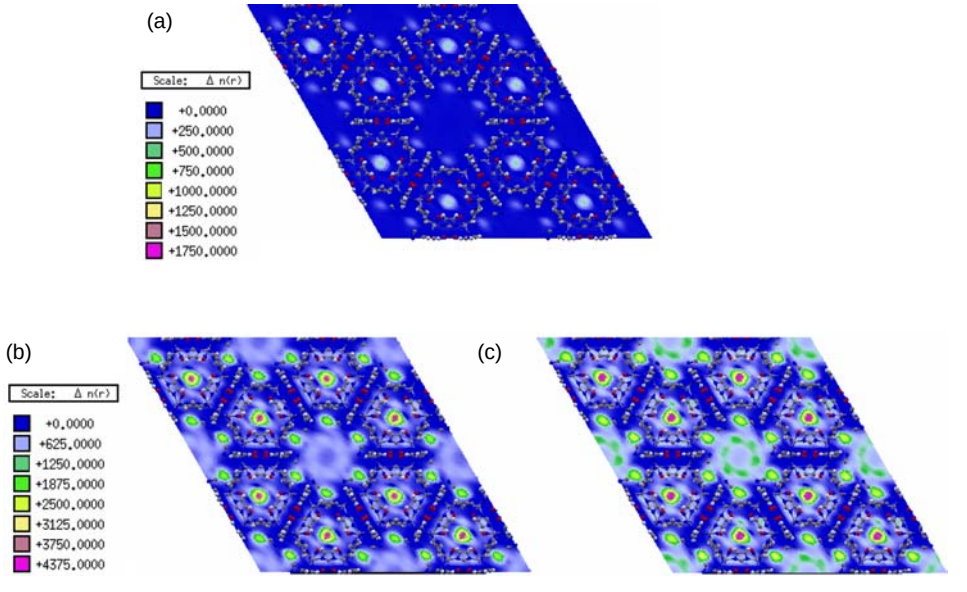

Figure 8. Probability distribution plots of COM of CH_4 in *XY* planes in ZIF-82 at different pressures: (a) 0.05 MPa, (b) 3.5 MPa and (c) 10.0 MPa (Zn, grey-blue; O, red; C, grey; H, white; N, blue) (colour online).

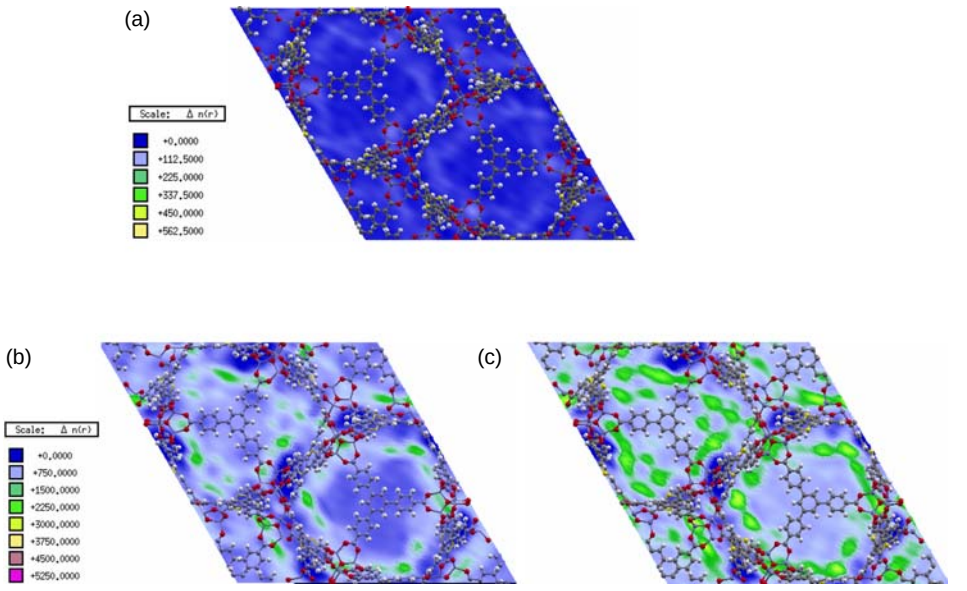

Figure 9. Probability distribution plots of COM of CH_4 in *XY* planes in UMCM-2 at different pressures: (a) 0.05 MPa, (b) 3.5 MPa, (c) 10.0 MPa (Zn, grey-blue; O, red; C, grey; H, white; N, blue; S, yellow) (colour online).

be more suitable for the modification to improve the methane storage capacity through increasing S_{acc} or V_{free}.

Acknowledgements

The financial support of the NSFC (Nos. 20725622, 20876006, 20821004, 20906002) is greatly appreciated.

References

[1] A. Celzard and V. Fierro, *Preparing a suitable material designed for methane storage: A comprehensive report*, Energy Fuels 19 (2005), pp. 573–583.
[2] D. Lozano-Castelló, J. Alcañiz-Monge, M.A. De la Casa-Lillo, D. Cazorla-Amorós, and A. Linares-Solano, *Advances in the study of methane storage in porous carbonaceous materials*, Fuel 81 (2002), pp. 1777–1803.
[3] C. Janiak, *Engineering coordination polymers towards applications*, Dalton Trans. 14 (2003), pp. 2781–2804.
[4] S. Kitagawa, R. Kitaura, and S. Noro, *Functional porous coordination polymers*, Angew. Chem. Int. Ed. 43 (2004), pp. 2334–2375.
[5] S.L. James, *Metal-organic frameworks*, Chem. Soc. Rev. 32 (2003), pp. 276–288.
[6] R.Q. Snurr, J.T. Hupp, and S.T. Nguyen, *Prospects for nanoporous metal-organic materials in advanced separation processes*, AIChE J. 50 (2004), pp. 1090–1095.
[7] T. Düren, L. Sarkisov, O.M. Yaghi, and R.Q. Snurr, *Design of new materials for methane storage*, Langmuir 20 (2004), pp. 2683–2689.
[8] S. Wang, *Comparative molecular simulation study of methane adsorption in metal-organic frameworks*, Energy Fuels 21 (2007), pp. 953–956.
[9] W. Zhou, H. Wu, and T. Yildirim, *Enhanced H_2 adsorption in isostructural metal-organic frameworks with open metal sites: Strong dependence of the binding strength on metal ions*, J. Am. Chem. Soc. 130 (2008), pp. 15268–15269.
[10] H. Wu, W. Zhou, and T. Yildirim, *High-capacity methane storage in metal-organic frameworks M_2(dhtp): The important role of open metal sites*, J. Am. Chem. Soc. 131 (2009), pp. 4995–5000.
[11] P.D.C. Dietzel, R. Blom, and H. Fjellvåg, *Base-induced formation of two magnesium metal-organic framework compounds with bifunctional tetratopic ligand*, Eur. J. Inorg. Chem. 23 (2008), pp. 3624–3632.
[12] S.R. Caskey, A.G. Wong-Foy, and A.J. Matzger, *Dramatic tuning of carbon dioxide uptake via metal substitution in a coordination polymer with cylindrical pores*, J. Am. Chem. Soc. 130 (2008), pp. 10870–10871.
[13] K. Koh, A.G. Wong-Foy, and A.J. Matzger, *A crystalline mesoporous coordination copolymer with high microporosity*, Angew. Chem. Int. Ed. 47 (2008), pp. 677–680.
[14] K. Koh, A.G. Wong-Foy, and A.J. Matzger, *A porous coordination copolymer with over 5000 m^2/g BET surface area*, J. Am. Chem. Soc. 131 (2009), pp. 4184–4185.
[15] A.P. Nelson, O.K. Farha, K.L. Mulfort, and J.T. Hupp, *Supercritical processing as a route to high internal surface areas and permanent microporosity in metal-organic frameworks materials*, J. Am. Chem. Soc. 131 (2009), pp. 458–460.
[16] R. Banerjee, A. Phan, B. Wang, C. Knobler, H. Furukawa, M. O'Keeffe, and O.M. Yaghi, *High-throughput synthesis of zeolitic imidazolate frameworks and application to CO_2 capture*, Science 319 (2008), pp. 939–943.
[17] R. Banerjee, H. Furukawa, D. Britt, C. Knobler, M. O'Keeffe, and O.M. Yaghi, *Control of pore size and functionality in isoreticular zeolitic imidazolate frameworks and their carbon dioxide selective capture properties*, J. Am. Chem. Soc. 31 (2009), pp. 3875–3877.
[18] N.L.C. Rosi, B.L. Chen, M. O'Keeffe, and O.M. Yaghi, *Rod-packings and metal-organic frameworks constructed from rod-shaped secondary building units*, J. Am. Chem. Soc. 127 (2005), pp. 1504–1518.
[19] P.D.C. Dietzel, Y. Morita, R. Blom, and H. Fjellvåg, *An* in situ *high-temperature single-crystal investigation of a dehydrated metal-organic framework compound and field-induced magnetization of one-dimensional metal-oxygen chains*, Angew. Chem. Int. Ed. 44 (2005), pp. 6354–6358.

[20] P.D.C. Dietzel, B. Panella, M. Hirscher, R. Blom, and H. Fjellvåg, *Hydrogen adsorption in a nickel based coordination polymer with open metal sites in the cylindrical cavities of the desolvated framework*, Chem. Commun. (2006), pp. 959–961.
[21] Accelrys, Inc., *Materials Studio, 3.1 V*, Accelrys, Inc., San Diego, CA, 2003.
[22] M.G. Martin and J.I. Siepmann, *Transferable potentials for phase equilibria. 1. United-atom description of n-alkanes*, J. Phys. Chem. B 102 (1998), pp. 2569–2577.
[23] A.K. Rappé, C.J. Casewit, K.S. Colwell, W.A. Goddard, III, and W.M. Skiff, *UFF, a full periodic table force field for molecular mechanics and molecular dynamics simulations*, J. Am. Chem. Soc. 114 (1992), pp. 10024–10035.
[24] G. Garberoglio, A.I. Skoulidas, and J.K. Johnson, *Adsorption of gases in metal organic materials: Comparison of simulations and experiments*, J. Phys. Chem. B 109 (2005), pp. 13094–13103.
[25] V. Krungleviciute, K. Lask, L. Heroux, A.D. Migone, J.Y. Lee, J. Li, and A. Skoulidas, *Argon adsorption on $Cu_3(BTC)_2(H_2O)_3$ (BTC = benzene-1,3,5-tricarboxylate) metal-organic framework*, Langmuir 23 (2007), pp. 3106–3109.
[26] A.I. Skoulidas and D.S. Sholl, *Self-diffusion and transport diffusion of light gases in metal-organic framework materials assessed using molecular dynamics simulations*, J. Phys. Chem. B 109 (2005), pp. 15760–15768.
[27] A.I. Skoulidas, *Molecular dynamics simulations of gas diffusion in metal-organic frameworks: Argon in CuBTC*, J. Am. Chem. Soc. 126 (2004), pp. 1356–1357.
[28] S. Keskin and D.S. Sholl, *Screening metal-organic framework materials for membrane-based methane/carbon dioxide separations*, J. Phys. Chem. C 111 (2007), pp. 14055–14059.
[29] R. Babarao, Z. Hu, J. Jiang, S. Chempath, and S.I. Sandler, *Storage and separation of CO_2 and CH_4 in silicalite, C_{168} schwarzite, and IRMOF-1: A comparative study from Monte Carlo simulation*, Langmuir 23 (2007), pp. 659–666.
[30] D. Frenkel and B. Smit, *Understanding Molecular Simulation: From Algorithms to Applications*, 2nd ed., Academic Press, San Diego, CA, 2002.
[31] Q. Yang, C. Zhong, and J. Chen, *Computational study of CO_2 storage in metal organic frameworks*, J. Phys. Chem. C 112 (2008), pp. 1562–1569.
[32] H. Frost, T. Düren, and R.Q. Snurr, *Effects of surface area, free volume, and heat of adsorption on hydrogen uptake in metal-organic frames*, J. Phys. Chem. B 110 (2006), pp. 9565–9570.
[33] D. Liu, C. Zheng, Q. Yang, and C. Zhong, *Understanding the adsorption and diffusion of carbon dioxide in zeolitic imidazolate frameworks: A molecular simulation study*, J. Phys. Chem. C 113 (2009), pp. 5004–5009.